


Rotor imbalance detection and quantification in wind turbines via vibration analysis

Wind Engineering
2022, Vol. 46(1) 3–11
© The Author(s) 2021
Article reuse guidelines:
sagepub.com/journals-permissions
DOI: 10.1177/0309524X21999841
journals.sagepub.com/home/wie


Jin Xu¹, Xian Ding¹, Yongli Gong¹, Ning Wu²  and Huihuang Yan²

Abstract

Rotor imbalance is a common fault in wind turbines, which may enhance radial loads that induce faults on the main bearing and gearbox. It usually results from the asymmetry of the air dynamics caused by blade crack, icing, etc. A simple and effective method on rotor imbalance detection and quantification is presented using the vibration signal collected from the accelerometer monitoring the wind turbine drive train. A vibration model describing the rotor imbalance under blade crack is proposed. The complex morlet wavelet transform is applied to the detection of the rotational frequency of rotor hub which represents the rotor hub. A health indicator that can quantify the degree of the rotor imbalance is designed. The proposed methods have successfully detected and quantified the rotor imbalance caused by blade crack in an on-site wind turbine.

Keywords

Wind turbine blades, rotor imbalance, complex wavelet transform, fault detection and quantification

Introduction

The rapid growth of wind energy has elevated the importance of reliability and safety of wind turbines as they impact operations cost and power efficiency. Wind turbines are conventionally located at remote area and exposed to harsh working environment, consequently they are subject to frequent failures (Ribrant and Bertling, 2007). It has been reported that operations and maintenance (O&M) cost of wind turbines accounts for 20% or more of the overall wind power generation cost (Igba et al., 2015).

Rotor hub of wind turbine is a significant part converting wind energy to mechanical energy. Three blades are installed on the rotor hub with pitch systems. Rotor hub is prone to be imbalance due to the asymmetry of air dynamics caused by blades icing, lightning burning, crack, etc. Once the rotor hub is imbalance, the additional centrifugal force increases, which enhances the load of the main bearing. This load may induce main bearing failure, even the secondary damage of planetary stage of wind turbine gearbox. Therefore, it is an urgent task to timely detect the rotor imbalance and judge the imbalance degree in order to eliminate the fault causes, avoiding the catastrophic result.

Many studies has been proposed to directly inspect blade faults that may result in rotor imbalance, which included non-destructive test (Amenabar et al., 2011), acoustic emission (Joosse et al., 2002; Liu et al., 2020; Tang et al., 2016), and infrared thermal image (Yan et al., 2004). The equivalent damage loading that may result in the occurrence of fatigue were also investigated in (Freebury and Musial, 2000). Ghoshal et al. (2000) judged whether the skin of blade is falling out through inspecting whistling. Wang and Zhang (2017) proposed a data-driven framework to automatically detect wind turbine blade surface cracks based on images taken by unmanned aerial vehicles (UAVs). Zhang and Jackman (2013) used an optical inspection method to detect wind turbine blade

¹China Green Development Investment Group Co., Ltd., Beijing, China

²Jiangsu Goldwind Science & Technology Co., Ltd., Yancheng, China

Corresponding author:

Ning Wu, 99, Jinhai Road, Dafeng Economic Development Zone, Yancheng 224100, Jiangsu, China.

Email: 17766171091@163.com

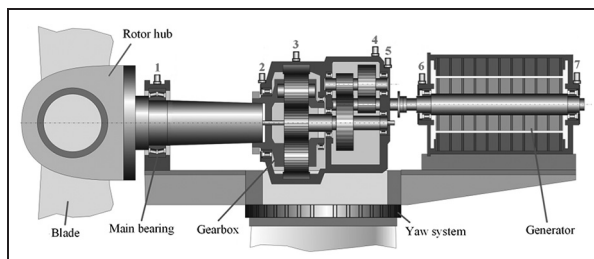


Figure 1. Vibration monitoring for wind turbine drive train.

surface crack, and found that the accuracy of quantifying a crack was improved by reducing noise with the intersection of two processed images from Sobel and Canny methods.

Analyzing the vibration signal from the transducer on the inner surface of the blade is another common method to find blade blades. Fitzgerald et al. (2010) developed a time-frequency based algorithm to detect damage in wind turbine blades from blade vibration signals, and considered the rotational speed of the blades and the stiffness of the blades and the nacelle. Tsai et al. (2009) proposed a continuous wavelet transform based entropy method to enhance the damage-detection capability of wind turbine blades, the approach can form a quantitative index systematically to detect the damage of blades, anticipating formulating a forewarning mechanism for wind power system. Zhao et al. (2015) applied the basic theory and algorithm of wavelet analysis and support vector machine (SVM) to extract the feature vector of the fault vibration signal of the blade in wind turbine, which obtained a good effect on identification of the blade crack damage. The above methods are effective in blade fault detection, but additional devices are needed that will enhance the hardware cost. Vibration analysis is a popular tool which is adopted to mainly monitor the health status of the drive train of wind turbine, involving the main bearing, gearbox, and generator. Gradually, it is a standard configuration equipped in modern wind turbine. However, the work using vibration signal from drive train to detect rotor imbalance was seldom reported.

The aim of this paper is to realize rotor imbalance detection and quantification only by analyzing the vibration signal from main bearing of wind turbine without any other extra monitoring devices. A vibration model describing rotor imbalance under blade faults is presented. Complex morlet wavelet transform is utilized to detect the rotational frequency of the rotor hub representing the rotor balance. A health indicator that can quantify the imbalance degree is proposed. An on-site wind turbine case with blade crack verifies the effectiveness of the proposed method. The method can help mechanic make reasonable maintenance schedule.

Vibration monitoring for wind turbine drivetrain

For horizontal axis wind turbines, stochastic winds are absorbed by blades and wind energy is converted into mechanical energy of rotor hub with low rotational speed, then the low rotational speed is speeded up through a gearbox to drive the generator in high speed. The blades and rotor hub are supported by main bearing. The rotor hub, main shaft, gearbox, and generator form the drive train. Several accelerometers are attached on different positions to monitor the health status of the drive train, shown as in Figure 1.

For the accelerometer 1 in Figure 1, it not only can monitor the status of main bearing, but is beneficial to analyze the balance of the rotor system, because it is the closest one near the rotor hub.

Vibration model of rotor imbalance with faulty blade

Vibration signal is the reflection of the health status of wind turbine blades and drivetrain. Through processing the vibration signal collected from the drivetrain, a quantity of faults, for example, rotor imbalance, gears or bearings crack, etc., can be detected. In view of this, the fault characteristics hidden in vibration signal need to be analyzed first.

Take the rotor imbalance with faulty blade as an example. A faulty blade will inevitably cause the change of aerodynamics itself, with a large difference on lift and drag relative to the other two healthy ones. Under this situation, the rotor imbalance is consequent. In Figure 2(a), the blade with crack is in front of the tower. When the faulty blade rotates $4\pi/3$ as shown in Figure 2(b), the vibration caused by rotor imbalance varies $4\pi/3$ as well, denoted by the red sinusoidal line. Additionally, each blade passes the tower will cause regular vibration, named

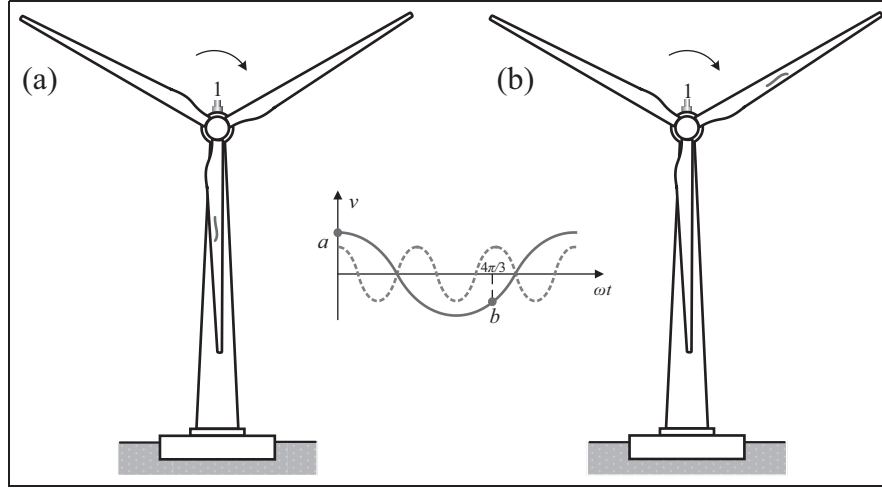


Figure 2. Vibration model of rotor imbalance with faulty blade. (a) cracked blade at vertical position, (b) after rotating $4\pi/3$ of the cracked blade.

tower effect, the frequency of which is three times of the rotational frequency of the rotor hub. The vibration caused by tower effect is a normal phenomenon, shown as the blue dash sinusoidal line in Figure 2.

In light of the aforementioned analysis, the vibration model can be deduced as

$$v(t) = \sum_{m=1}^M A_m \sin(m \cdot \omega t + \varphi_m) + \sum_{n=1}^N A_n \sin(3 \cdot n \cdot \omega t + \varphi_n) \quad (1)$$

where, the first item in the right side is caused by rotor imbalance, and the second item in the right side is caused by tower effect. A_m is the m th order vibration amplitude caused by rotor imbalance, A_n is the n th order vibration amplitude caused by tower effect, ω is the rotational speed of the rotor hub, and φ_m and φ_n are the m th order and n th order initial phases of each vibration component.

Fault detection and quantification using complex wavelet transform

Complex wavelet transform

The vibration information in equation (1) usually modulates the resonance frequency of fundamental structure or the other frequencies. Thus demodulation analysis for the vibration signal to obtain the fault characteristic frequency is necessary.

Complex wavelet transform is an effective demodulation method that can simultaneously realize filtering signals at different bandwidth and multi-scale envelope representation. It needs not human interference to select filter bands, thus it is simple and applicable.

Complex wavelet has the property of being analytic in nature, which is defined as.

$$\psi(t) = \psi_R(t) + j\psi_I(t) = \psi_R(t) + jH[\psi_R(t)] \quad (2)$$

where $\psi_R(t)$ is the real part of complex wavelet, $\psi_I(t)$ is the imaginary part of the complex wavelet, and $\psi_I(t)$ is the Hilbert transform of $\psi_R(t)$. Figure 3 shows the complex morlet wavelet used in this paper.

The complex wavelet transform of vibration signal $x(t)$ is

$$wt_C(a, \tau) = wt_R(a, \tau) + j wt_I(a, \tau) \quad (3)$$

where

$$\begin{cases} wt_R(a, \tau) = |a|^{-1/2} \int_{-\infty}^{\infty} x(t) \psi_R^*\left(\frac{t-\tau}{a}\right) dt \\ wt_I(a, \tau) = |a|^{-1/2} \int_{-\infty}^{\infty} x(t) H[\psi_R^*\left(\frac{t-\tau}{a}\right)] dt \end{cases} \quad (4)$$

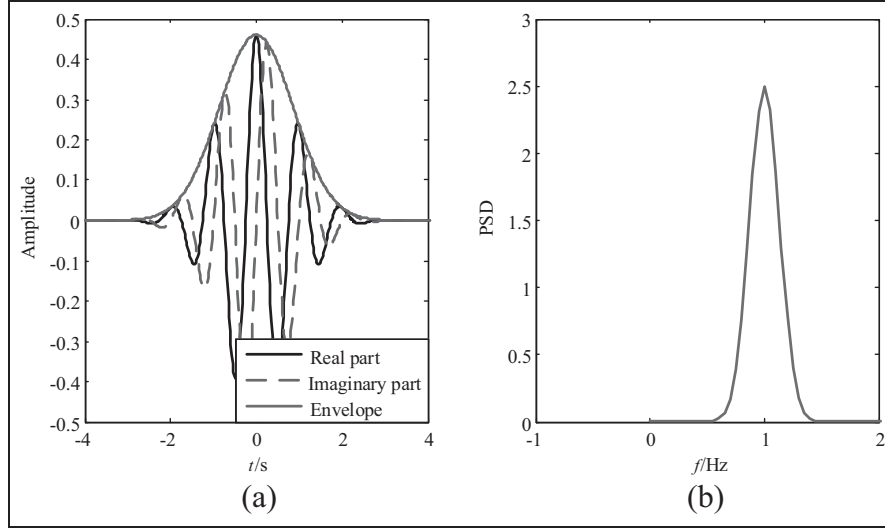


Figure 3. Complex morlet wavelet. (a) wavelet waveform, (b) power spectrum density of complex morlet wavelet.

In equations (3) and (4), a is the scale factor and τ represents the shift factor.

The result after complex wavelet transform is analytic. From the modulus of the analytic result $wt_C(a, \tau)$, the envelope signal is calculated as

$$\begin{aligned} e_{wt}(a, \tau) &= ||wt_C(a, \tau)|| \\ &= \sqrt{wt_R(a, \tau)^2 + H[wt_R(a, \tau)]^2} \end{aligned} \quad (5)$$

Therefore, the band-pass filtering and envelope analysis can be finished simultaneously.

Further, using Fourier transform, multi-scale envelope spectrogram (MuSenS) can be computed as

$$\begin{aligned} E_{wt}(a, f) &= F(||wt_C(a, \tau)||) \\ &= \frac{1}{2\pi} \int_{-\infty}^{\infty} ||wt_C(a, \tau)|| e^{-j2\pi f\tau} d\tau \end{aligned} \quad (6)$$

Fault detection and quantification

As the analysis in Section 3, the demodulation of rotational frequency of the rotor hub will indicate the rotor imbalance. However as we know, the vibration amplitude caused by rotor imbalance is proportional to the rotational speed of the rotor hub. Therefore, the degree of imbalance cannot be evaluated only by the vibration amplitude. Considering the tower effect (three times of the rotational speed of the rotor hub) is relevant to the rotational frequency of the rotor hub, the following indicator is proposed to quantify the degree of rotor imbalance.

$$Hi = \frac{DA(f_1, :) + DA(2f_1, :)}{DA(3f_1, :)} \quad (7)$$

where DA is demodulated amplitude of MuSenS using complex wavelet transform, f_1 is the rotational frequency of the rotor hub, $2f_1$ is twice harmonics of the rotational frequency, $3f_1$ is the pass frequency of the blades: means the summation computation of all the scales. The numerator in equation (7) denotes the fault information of rotor imbalance, and the denominator denotes the ordinary tower effect.

Case study

The tested wind turbine is a fixed-pitch one, the rated power of which is 750 kW. The wind turbine were tested four times in all. Among these, blade crack was found during the second test. The first test was implemented 1 year

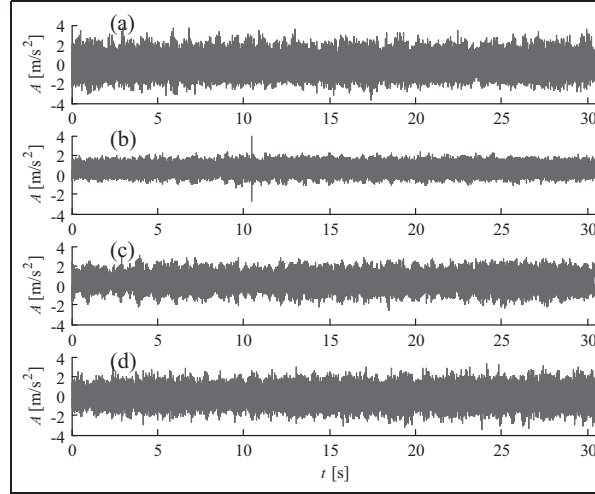


Figure 4. The vibration signals during the four tests: (a) the first test, (b) the second test, (c) the third test, and (d) the forth test.

before the second test. The third test was immediately carried after repairing the crack of the faulty blade. The forth test happened after the third one. The rotational frequency of the rotor hub was 0.362 Hz during the test. The test was offline, one accelerometer by one on the surface of the wind turbine drive train, shown as in Figure 1.

The sampling frequency of accelerometer 1, 2, and 3 in Figure 1 is 5120 Hz due to the relatively low rotational speed of the monitored parts, and the sampling frequency of the rest ones is 25,600 Hz. Figure 4 shows the vibration signals from accelerometer 1 during the four tests. Figure 4(a) to (c), and d correspond with the four vibration tests sequentially. All the vibration amplitudes in Figure 4 are in the range of $\pm 4 \text{ m/s}^2$, where the amplitude in the second test with blade crack is lower than the other tests. This brings an opposite result to the original viewpoint that faults will make vibration larger. The vibration signals are occupied by random vibration information, without prominent periodic or impact components. It is difficult to judge potential fault only by observing the vibration waveform.

The original vibration signals are processed using complex morlet wavelet transform, and the MuSenS is shown in Figure 5. The wavelet scale is from 10 to 25, and the step is 0.25. In the first test of Figure 5(a), the frequency 1.02 Hz corresponding to the tower effect of three blades passing the tower exists, but is tiny, which is hidden by stochastic vibration components, according with the health status of the rotor and blades at that time. The reason that the frequency 1.02 Hz is insufficient lies in the extra noise during testing. In Figure 5(b), 0.362 Hz and its harmonics are distinct, which corresponds to the rotational frequency of the rotor hub, indicating the rotor imbalance caused by blade fault. This results effectively verify the on-site situation that the blade was crack during the second test. Figure 5(c) shows the MuSenS after repairing the cracked blade, where only 1.053 Hz (three times of the rotational frequency of the rotor hub) is evident. The frequency 1.053 Hz accords with the tower effect of three blades passing the tower sequentially, which is an ordinary phenomenon demonstrating that the blade was repaired successfully at that time. Six month later, the fourth test was implemented, and the MuSenS using complex wavelet transform is shown in Figure 5(d). Here, the rotational frequency of the rotor hub disappears, indicating that the wind turbine keeps steady operation after repair.

The slice of the MuSenS at scale 25 is shown in Figure 6. We can clearly observe 0.362 Hz and its harmonics in Figure 6(b) when the blade is cracked. No matter before maintenance in Figure 6(a) or after maintenance in Figure 6(c) and (d), the rotational frequency of the rotor hub is insignificant. Once again, Figure 6 demonstrates the effectiveness of the proposed vibration model and MuSenS based demodulation method.

We pictured the cracked blade during the second test. The picture is shown in Figure 7. On account of this crack, the symmetry of the air dynamics of three blades were destroyed and the rotor imbalance emerged at that time. The MuSenS has successfully detected the rotor imbalance using vibration analysis.

The degree of rotor imbalance is quantified as equation (7) during the four vibration tests. The computed health indicator is shown in Figure 8, where we can see that the health indicator of the second test is higher than the other ones. Although the vibration amplitude in Figure 4(b) when blade is cracked (the second test) is lower than the other three healthy status, the health indicator is prominent in Figure 8, corresponding to the fact that the

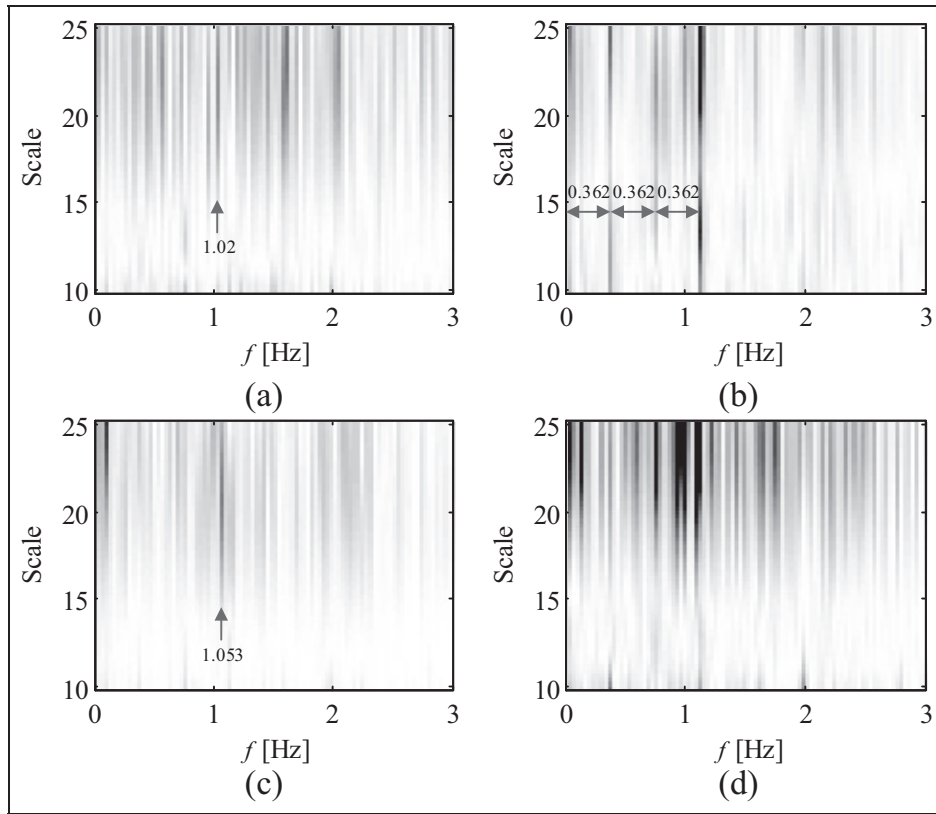


Figure 5. MuSEnS using complex wavelet transform. (a) the first test, (b) the second test, (c) the third test, and (d) the forth test.

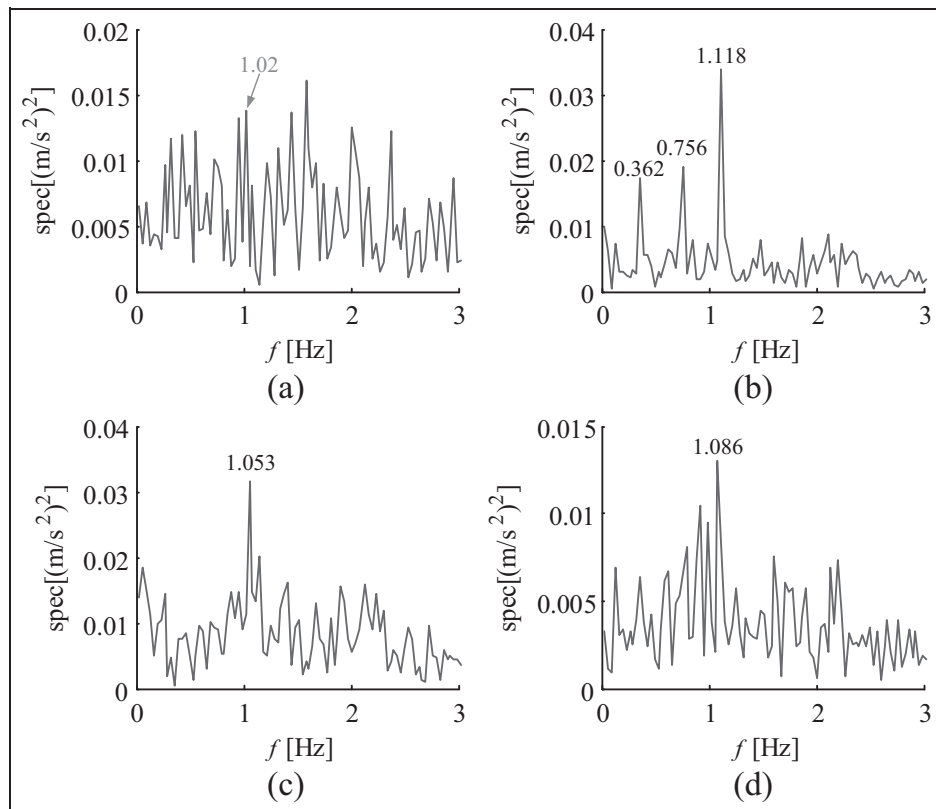


Figure 6. Slices of complex wavelet transform at scale = 25. (a) the first test, (b) the second test, (c) the third test, and (d) the forth test.



Figure 7. Crack in a blade of the tested wind turbine.

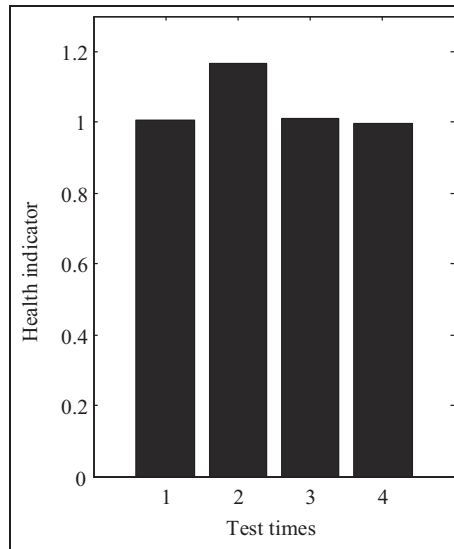


Figure 8. The health indicator during four tests.

amplitude of fault characteristic frequency increases under faulty status. By contrast, the health indicators before and after blade fault remain the similar level, accurately reflecting the healthy degree of the rotor imbalance.

Further, the frequency range is extended, and the MuSEnS is shown in Figure 9, where the low frequency including the rotational frequency of rotor hub cannot be evidenced due to the frequency scale. Nevertheless, around 30 Hz vibration frequency and its harmonics arise during the four tests in Figure 9 and its slice in Figure 10, which denotes the mesh frequency of the planetary gear set in the wind turbine gearbox. This is normal because the vibration source in gearbox can be delivered to accelerometer 1 through the main shaft.

Conclusion

Wind turbine blade faults are prone to induce rotor imbalance. A fault detection and quantification on rotor imbalance is proposed in this paper using vibration analysis. A vibration model of rotor imbalance under blade fault is constructed. Then the MuSEnS using complex morlet wavelet transform is applied to the rotor imbalance detection, and a health indicator that can quantify the degree of rotor imbalance is presented by the ratio of the vibration amplitude of rotational frequency to the third harmonics.

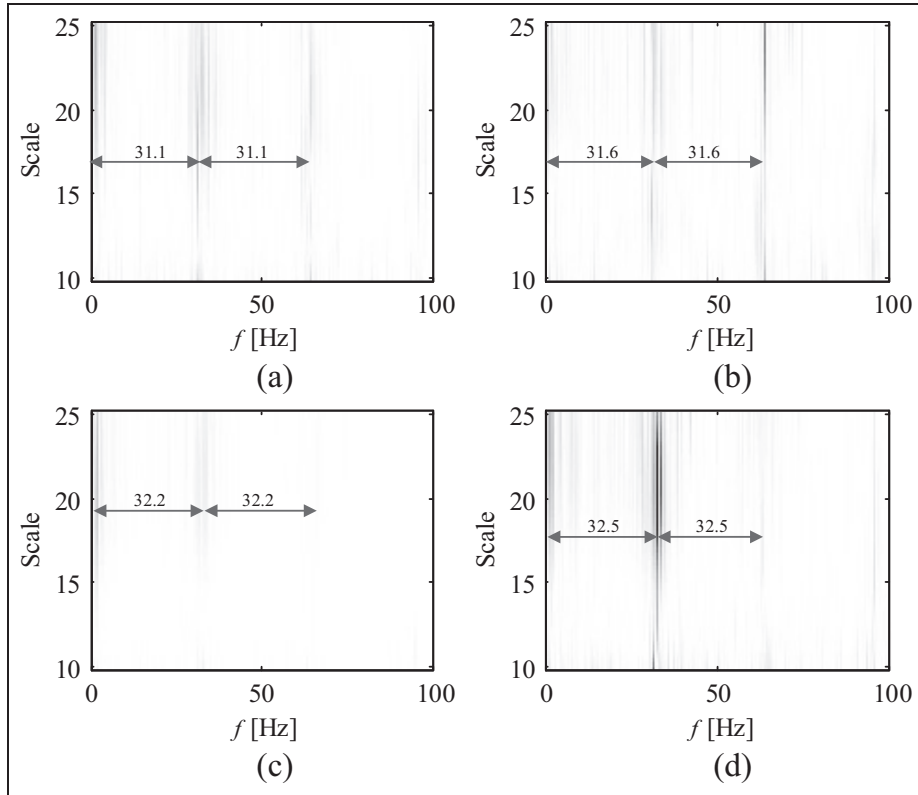


Figure 9. MuSEnS using complex wavelet transform. (a) the first test, (b) the second test, (c) the third test, and (d) the forth test.

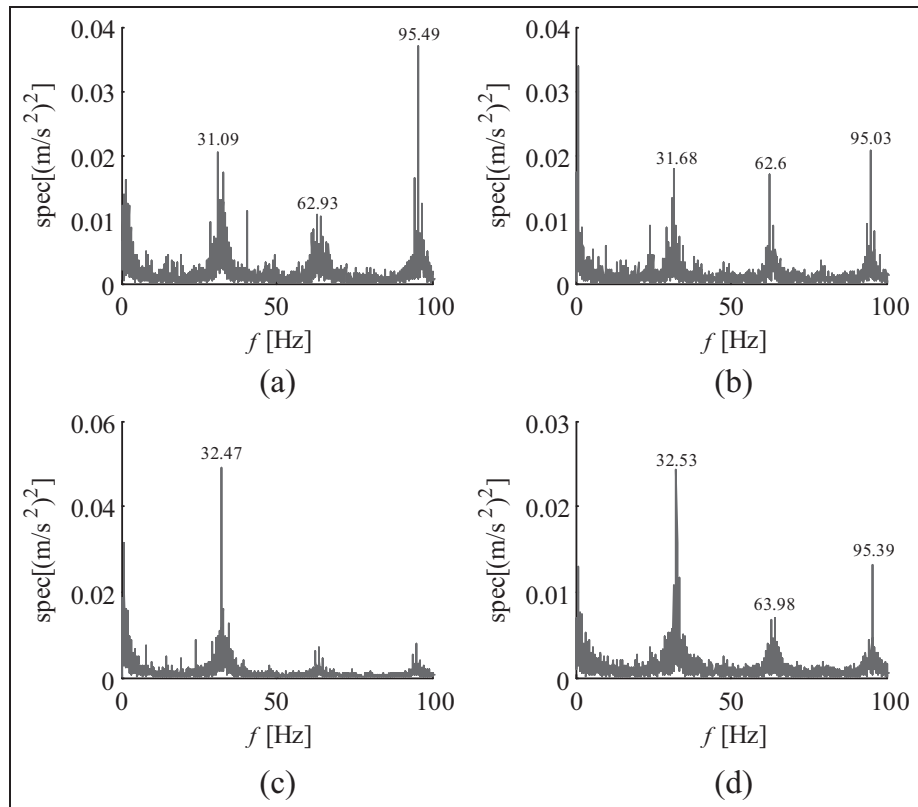


Figure 10. Slices of complex wavelet transform at scale = 25. (a) the first test, (b) the second test, (c) the third test, and (d) the forth test.

A 750 kW wind turbine with blade fault is tested four times by the proposed method. The tested results show that the proposed fault detection and quantification method is simple and effective for judging rotor imbalance.

Declaration of conflicting interests

The author(s) declared no potential conflicts of interest with respect to the research, authorship, and/or publication of this article.

Funding

The author(s) received no financial support for the research, authorship, and/or publication of this article.

ORCID iD

Ning Wu  <https://orcid.org/0000-0002-0095-9233>

References

- Amenabar I, Mendikute A, Lopez-Arraiza A, et al. (2011) Comparison and analysis of non-destructive testing techniques suitable for delamination inspection in wind turbine blades. *Composites Part B* 42(5): 1298–1305.
- Fitzgerald B, Arrigan J and Basu B (2010) Damage detection in wind turbine blades using time-frequency analysis of vibration signals. In: *IEEE international joint conference on neural networks*, Barcelona, Spain, 18–23 July, pp.1–5.
- Freebury G and Musial W (2000) Determining equivalent damage loading for full-scale wind turbine blade fatigue tests. In: *The 19th American Society of Mechanical Engineers (ASME) wind energy symposium*, Reno, NV, USA, 10–13 January.
- Ghoshal A, Sundaresan M, Schulz M, et al. (2000) Structural health monitoring techniques for wind turbine blades. *Journal of Wind Engineering and Industrial Aerodynamics* 85(3): 309–324.
- Igba J, Alemzadeh K, Henningsen K, et al. (2015) Effect of preventive maintenance intervals on reliability and maintenance costs of wind turbine gearboxes. *Wind Energy* 18(11): 2013–2024.
- Joose P, Blanch M, Dultton A, et al. (2002) Acoustic emission monitoring of small wind turbine blades In: *ASME wind energy symposium, aerospace sciences meetings*, Reno, NV, USA, 14–17 January, pp.400–406.
- Liu Z, Wang X and Zhang L (2020) Fault diagnosis of industrial wind turbine blade bearing using acoustic emission analysis. *IEEE Transactions on Instrumentation and Measurement* 69(9): 6630–6639.
- Ribrant J and Bertling LM (2007) Survey of failures in wind power systems with focus on Swedish wind power plants during 1997–2005. *IEEE Transactions on Energy Conversion* 22: 167–173.
- Tang J, Soua S, Mares C, et al. (2016) An experimental study of acoustic emission methodology for in service condition monitoring of wind turbine blades. *Renewable Energy* 99(12): 170–179.
- Tsai CS, Hsieh CT and Lew KL (2009) Detection of wind turbine blades damage by spectrum-recognition using Gaussian wavelet-entropy. In: *International conference on anti-counterfeiting*, Hong Kong, China, 20–22 August, pp.108–113. New York, NY: IEEE Press.
- Wang L and Zhang Z (2017) Automatic detection of wind turbine blade surface cracks based on UAV-taken images. *IEEE Transactions on Industrial Electronics* 64(9): 7293–7303.
- Yan T, Smith G, Clayton B, et al. (2004) Infrared thermography for non-destructive testing of wind turbine blades. In: *The 3rd world wind energy conference and renewable energy*, Beijing, China, 1 October–4 November.
- Zhang H and Jackman J (2013) A feasibility study of wind turbine blade surface crack detection using an optical inspection method. In: *IEEE international conference on renewable energy research & applications*, Madrid, Spain, 20–23 October, pp.20–23.
- Zhao Q, Li W, Shao Y, et al. (2015) Damage detection of wind turbine blade based on wavelet analysis. In: *2015 8th International Congress on Image and Signal Processing (CISP)*, Shenyang, China, 14–16 October, pp.1406–1410. New York, NY: IEEE.